Biometals
DOI 10.1007/s10534-016-9972-y

After oxidation, zinc nanoparticles lose their ability to enhance responses to odorants

Samantha Hagerty · Yasmine Daniels · Melissa Singletary · Oleg Pustovyy · Ludmila Globa · William A. MacCrehan · Shin Muramoto · Gheorghe Stan · June W. Lau · Edward E. Morrison · Iryna Sorokulova · Vitaly Vodyanoy

Received: 19 July 2016 / Accepted: 9 September 2016

Abstract Electrical responses of olfactory sensory neurons to odorants were examined in the presence of zinc nanoparticles of various sizes and degrees of oxidation. The zinc nanoparticles were prepared by the underwater electrical discharge method and analyzed by atomic force microscopy and X-ray photoelectron spectroscopy. Small (1.2 ± 0.3 nm) zinc nanoparticles significantly enhanced electrical responses of olfactory neurons to odorants. After oxidation, however, these small zinc nanoparticles were no longer capable of enhancing olfactory responses. Larger zinc oxide nanoparticles (15 nm and 70 nm) also did not modulate responses to odorants. Neither zinc nor zinc oxide nanoparticles produced olfactory responses when added without odorants. The enhancement of odorant responses by small zinc nanoparticles was explained by the creation of olfactory receptor dimers initiated by small zinc nanoparticles. The results of this work will clarify the mechanisms for the initial events in olfaction, as well as to provide new ways to alleviate anosmia related to the loss of olfactory receptors.

Keywords Olfaction · Olfactory receptors · Electroolfactogram · Perception · XPS · TEM · AFM

S. Hagerty · M. Singletary · O. Pustovyy · L. Globa · E. E. Morrison · I. Sorokulova · V. Vodyanoy
Department of Anatomy, Physiology and Pharmacology, Auburn University College of Veterinary Medicine, Auburn, AL, USA

Y. Daniels · W. A. MacCrehan · S. Muramoto · G. Stan · J. W. Lau
Material Measurement Laboratory, National Institute of Standards and Technology, Gaithersburg, MD, USA

V. Vodyanoy (✉)
Auburn University, 109 Greene Hall, Auburn, AL 36849, USA
e-mail: vodyavi@auburn.edu

Introduction

Previous studies have demonstrated that zinc metal nanoparticles, at low concentrations, can enhance electroolfactogram (EOG) or whole cell patch-clamp responses to odorants (Viswaprakash et al. 2006, 2009). Introducing these particles along with an odorant can increase responses by about 3-fold. Zinc nanoparticles, create no odor effects alone, but increase the odor response if mixed with an odor. In small concentrations, effects are dose-dependent and reversible. The particles are spontaneously eliminated from the olfactory mucosa; providing a specific, sensitive, and efficient way of olfactory response control. Some other metal nanoparticles such as copper, gold, and silver do not present the results observed for zinc. Gold and silver nanoparticles created a transient enhancement, while copper nanoparticles did not affect the relative EOG

Published online: 20 September 2016

amplitude, but prolonged the overall stability of the signals (Viswaprakash et al. 2009). When zinc nanoparticles were replaced by Zn^{2+} ions at the same concentrations, a decrease in receptor neuron response was recorded. When the enzymatic decomposition of the second messenger cyclic adenosine monophosphate (cAMP) was eliminated by the membrane-permeable phosphodiesterase inhibitor 3-isobutyl-1-methylxanthine (IBMX), the increased cAMP produced EOG signals that were not enhanced by zinc nanoparticles (Moore et al. 2012). Based on these findings, we determined that zinc nanoparticles function at the olfactory receptor level and engage in the initial events of olfaction. A kinetic model of olfactory receptor/odorant/metal interactions based upon experimental results described a stoichiometry of metal nanoparticles and receptors, and the mode of their action (Vodyanoy 2010). The kinetic olfactory model estimated that one metal nanoparticle binds two receptor molecules to make a dimer. Our canine functional magnetic resonance imaging (fMRI) results indicate that the addition of zinc nanoparticles results in a significant increase of brain excitation in response to odorants, consistent with the increase in excitation of olfactory sensory neurons observed in response to higher vs. lower concentrations of odorants (Jia et al. 2012, 2014, 2016). These results agree well with our in vitro electrophysiological results. We showed that most of the atoms of small zinc nanoparticles were not oxidized (Vodyanoy et al. 2016). In the present work, we will examine the effect of zinc nanoparticles oxidation on their ability to enhance odorant responses. Furthermore, we will determine if zinc oxide nanoparticles evoke significant responses in olfactory sensory neurons when delivered without odorants.

Methods

Metal nanoparticles

Metal nanoparticles were produced by a modified method (Kruyt 1952; Tokushige et al. 2010). The system consists of a water container, having a high-voltage generator connected to two metal electrodes submerged in water. By controlling the voltage and distance between electrodes, the plasma created under water produces a very fine dispersion of the metal into nanoparticles. Two metal electrodes (Alfa Aesar, 99.9999 %) of 2 mm diameter are positioned in a large Pyrex jar ≈7 mm below the gas–water interface at the distance between electrodes of ≈0.5 cm. 750 mL of LC–MS grade water (Omnisolv) are used in this procedure. Before the experiment, to remove dissolved oxygen, the water was heated up to boiling point and boiled until the large vapor bubbles appeared. The water then cooled to 298.15 K (25 °C) and for 20 min percolated with nitrogen gas produced by evaporation of liquid nitrogen. The jar filled with nitrogen gas was placed in the water bath with running water to prevent overheating. An alternating voltage of 15 kV and 60 Hz, was applied to the electrodes, and the electric discharge was sustained for 1 h. The water suspension was collected in a 1 L glass beaker and placed in the refrigerator for 12 h to allow large metal particles to sediment. Suspended particles were separated from the sediment and subjected to centrifugation at 147,099.75 m/s^2 (15,000 g_n) for 2 h at 298.15 K (25 °C). After centrifugation, the pellet was discarded, and the supernatant was subjected to further centrifugations to produce fractions of nanoparticles enriched in particles of particular sizes. The centrifuge speed and time to separate nanoparticles by size was estimated with Stock's equation.

$$U = g_n d^2 (D - \rho)/18\eta,$$

where U was the rate of sedimentation, g_n—acceleration, d—diameter of the nanoparticle, D and ρ are densities of metal and water, respectively, and η is the viscosity of water.

Zinc nanoparticles were size-selected for 1 nm to 2 nm diameters. These were prepared by the electrical discharge method as described above, a part of the small zinc nanoparticles was oxidized by percolating air through the suspension of nanoparticles for 20 min at 313.15 K (40 °C). The air for the oxidation procedure was obtained by evaporation of liquid air. Zinc oxide nanoparticles provided by NIST with nominal diameters of 15 nm to 70 nm (Black et al. 2012; Cline et al. 2013) were also used in olfactory experiments.

The particle suspensions were analyzed similarly to methods described previously (Samoylov et al.

2005; Daniels et al. 2015; Vodyanoy et al. 2016). The total concentration of metal in suspension was measured by atomic absorption spectra (GTW Analytical Services), and the particle size and number determined by the atomic force microscopy (AFM). The crystallinity of small nanoparticles was analyzed by the transmission electron microscopy (TEM). The degree of nanoparticle oxidation was obtained from the X-ray photon spectroscopy (XPS).

Zn^{2+} ion concentration in suspensions of nanoparticles

Zinc ion concentration was measured in the zinc and zinc oxide nanoparticle water suspension. The concentration of Zn^{2+} ions in suspensions of small zinc nanoparticles was measured before and after oxidation. Zn^{2+} measurements were carried out with duplicate samples. Zinc ion levels were measured using the Colorimetric Zinc Ion Quantitation Kit (AAT Bioquest, Sunnyvale, CA) according to the manufacturer's instructions. Optical density values were measured at 620 nm using a microplate reader (Bio-Tek, Winooski, VT). The zinc ion concentration of the sample was determined by comparison of experimental mean values with curves generated by standards, supplied with the assay. The minimum detectable concentration of the assay was 0.1 μmol/L.

TEM

TEM was performed using an FEI Titan at 300 kV. A few microliters of air-dried droplets of the Zn NP suspension were spread onto a holey carbon substrate on copper TEM grids. Fringes widths were measured on different nanoparticles, and the Miller-Bravais indices of the crystalline structures were calculated using the Crystallography lab software (Gu et al. 2016).

AFM

Images of metal nanoparticles were taken by Bruker MultiMode 8 (Santa Barbara, CA) atomic force microscope in Tapping® (intermittent-contact) mode, using PPP-SEIH Nanosensors (Neuchatel, Switzerland) AFM probes; the nominal values specified by the vendor for the force constant and the resonance frequency of these probes are 15 N/m and 130 kHz, respectively. The AFM calibration was verified before measurements on crystallographic 6H-SiC (0001) steps. From the topographical micrographs of these steps, the AFM calibration was found to be within 3 % accuracy of the nominal height (0.75 nm) of SiC single half-monolayers. The AFM imaging was used to measure the size distribution of particles. Monolayers of zinc nanoparticles were prepared on a mica substrate for all measurements by depositing and evaporating a small amount of 0.01 % nanoparticles water suspension on freshly cleaved mica surfaces.

XPS

XPS was used to make quantitative spectroscopic measurements of the elemental composition of the nanoparticles' surfaces. The Kratos Axis Ultra delay-line detector (DLD) instrument in the hybrid mode used a monochromatic Al Kα1, 2 X-ray source ($h\upsilon = 1486.6$ eV). The stoichiometry of the Zn and ZnO components were determined from the high-resolution spectra of Zn 2p (1017 eV to 1057 eV) and were acquired using a pass energy of 40 eV with an energy resolution of 0.1 eV. A Gaussian distribution was used for peak fitting, with a full width at half maximum (FWHM) constraint of 1.7 eV, which was obtained from the C 1 s peak located at 285 eV (BE). Water suspensions containing zinc and zinc oxide nanoparticles were deposited separately on silicon wafers and allowed to evaporate during pump down to minimize oxidation. To examine the stability of zinc metal nanoparticles, the particles were stored at 278 K (5 °C) for 317 days and XPS were measured at the beginning and the end of the storage.

Animals

Animals used in this project were cared for by the Division of Laboratory Animal Health of Auburn University assuring compliance with all applicable regulations. The primary regulations governing the care and use of animals utilized in research and teaching include the following: the Animal Welfare Act, the NIH-PHS Policy, the Guide for the Care and Use of Laboratory Animals, and the Guide for the Care and Use of Agricultural Animals in Agricultural Research and Teaching. The protocol was approved by the Auburn University Institutional Animal Care and Use Committee (AU IACUC) committee. Strong efforts were made to avoid exposing animals to

discomfort, pain, or injury. Adult male Sprague-Dawley rats (Envigo, Dublin, VA) weighing 250 g to 300 g were used.

Odorants

Odorants were purchased from Sigma-Aldrich. An odorant mixture containing 1.6 mmol/L each of ethyl butyrate, eugenol, and (+) and (−) carvone in water was mixed with a vortex and stored in a dark glass bottle until the experiment.

Delivery of odorants and metal nanoparticles

For stimulation, a 0.25 s pulse of the odorant mixture at 55158 N/m^2 (8 psi) was formed by a computer-controlled Pneumatic PicoPump PV800 (World Precision Instruments, Sarasota, FL). A pulse of positive pressure drove the odorant into a glass nozzle directed at the olfactory epithelium (OE). The residual odorant was cleared by air between each stimulus application. The odorant pulse patterns were initiated manually at predetermined time intervals or automatically by a computer. The automatic computer routine was composed of 0.25 s pulses at 20 s and 60 s intervals for EOG recording. One series of 10 pulses at 20 s intervals constituted one ''EOG recording''. Thus, in the automatic regime, the single EOG recording had a duration of 200 s and could correspond to 10 response traces. These recordings were repeated as many times as needed to cover a desirable number of pulses and duration for a single experiment. A nanoparticle suspension was mixed with odorant solutions to make final nanoparticle concentrations of 0.02 nmol/L. During the puff, the odorant vapor containing metal nanoparticles was delivered to the OE surface. We showed that delivery of metal nanoparticles by the water vapor and the liquid suspension produced an efficient transfer of particles to the OE (Viswaprakash et al. 2009). The odorants and nanoparticles delivered by the water vapors were perceived by live animals (Jia et al. 2014, 2016).

Electrophysiology

Our measurements are based on electroolfactography (EOG) (Viswaprakash et al. 2009). The method utilizes Axon Instrument MultiClamp 700A amplifier and 1322A DigiData acquisition system.

Electroolfactogram (EOG)

Rat septal olfactory mucosa was dissected out and placed in a perfusion chamber such that the basal portions were immersed in physiological buffer (containing 137 mmol/L NaCl, 5.3 mmol/L KCl, 4.2 mmol/L $NaHCO_3$, 0.4 mmol/L KH_2PO_4, 3.4 mmol/L Na_2HPO_4, 1.3 mmol/L $CaCl_2$, 0.2 mmol/L $MgSO_4$, and 5.6 mmol/L D-glucose at pH 7.4), while the epithelial surface with olfactory cilia was exposed to air. Patch electrodes of approximately 24 μm tip opening filled with the same physiological buffer were connected to a patch-clamp amplifier to detect responses from the OE. Once contact between the electrode and the surface of the OE was formed, air puffs of the odorant mixture were applied. Zinc metal or metal oxide particles were added to the odorant mixture. Odor responses over the time course of several minutes were recorded after being amplified by a patch-clamp amplifier and filtered at 2 kHz to 5 kHz. The stimuli were given by three sequences. The sequence I was composed of the pulses (1) odorant mixture, (2) odorant mixture +small zinc nanoparticles, (3) odorant mixture + 15 nm ZnO nanoparticles, (4) odorant mixture + 70 nm ZnO nanoparticles, (5) 15 nm ZnO nanoparticles, (6) 70 nm ZnO nanoparticles, and (7) water vapors. The sequence II contained pulses of (1) odorant mixture, (2) odorant mixture +small zinc nanoparticles, (3) odorant + small ZnO nanoparticles, (4, 5) water vapor. The sequence pulses III was applied to the olfactory and respiratory epithelia and composed of (1) odorant mixture, (2) odorant mixture +small zinc nanoparticles.

At one contact, 3–5 repetitions of the EOG recording of 10 traces each were collected. After completion of EOG recording in the first contact, the electrode was moved to another area of the OE and a new contact was made to generate 3–5 repetitions of EOG recording. EOG was collected from 3 to 5 areas of the epithelium and experiments were replicated with 2–3 epithelia for each sequence of pulses.

Results

AFM and XPS

Figure 1 exhibits the physical properties of zinc nanoparticles prepared by high-voltage discharge. AFM showed the size distributions of Zn

nanoparticles, with average diameters of 1.2 ± 0.3 nm (Fig. 1a). A histogram (Fig. 1b) shows a distribution with a relatively high peak around the average value [the standard deviation (SD) was calculated from the bell distribution around the peak] and the tail up to 6 nm. Figure 1c displays the XPS of freshly prepared (3 days old) 1.2 nm zinc nanoparticles. The XPS analysis of the Zn $2p_{3/2}$ core line revealed that metallic zinc nanoparticles were oxidized to a very small extent, where the relative atomic concentrations of Zn and ZnO species were determined to be [93.9 ± 3.4 (SD)] and [6.1 ± 3.4 (SD)] %, respectively. These data reveal that about 94 % of metal atoms were not oxidized. In contrast, the 1.2 nm zinc oxide nanoparticles were found to contain smaller concentrations of metallic zinc [88.5 ± 2.1 (SD)] % and a higher concentration of oxidized zinc [11.5 ± 2.1 (SD)] %, respectively. As expected, the 15 and 70 nm zinc oxide nanoparticles contained [98.2 ± 0.2 (SD)] and [99.3 ± 0.4 (SD)] % of ZnO, respectively. After 317 days of storage of 1.2 nm zinc nanoparticles at 278 K (5 °C), the XPS showed the relative atomic concentrations of Zn and ZnO species to be [96.0 ± 0.5 (SD)] and [4.0 ± 0.5 (SD)] %, respectively. The relative atomic concentrations at the beginning and the end of storage are not significantly different ($n = 6$, $p < 0.01$).

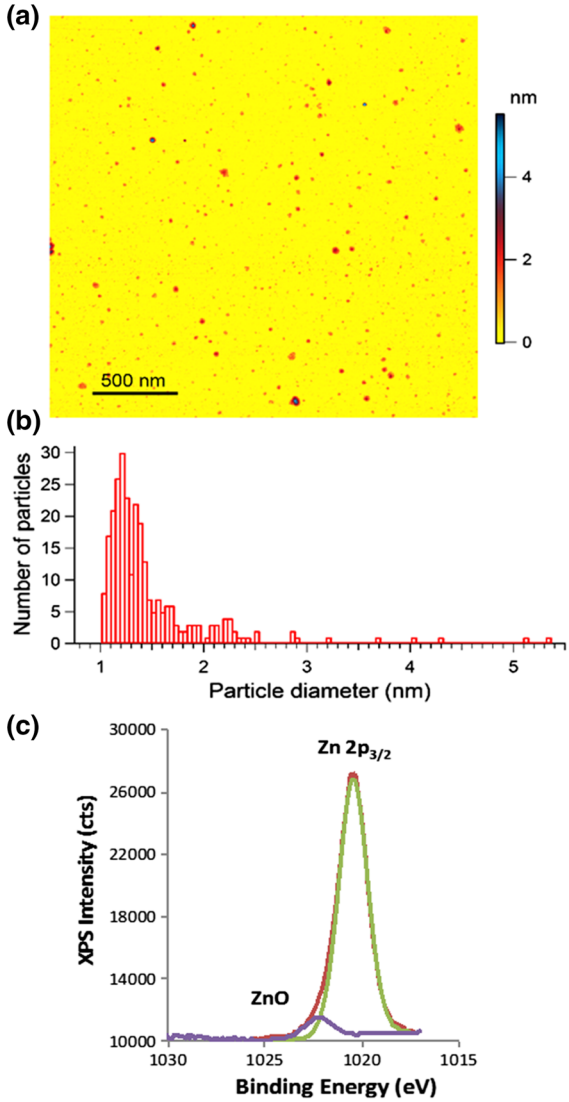

Fig. 1 Physical characterization of small zinc nanoparticles. **a** Atomic force microscope image, 0.01 % zinc nanoparticles on mica. 270 nanoparticles with height above 1 nm were detected over a 2.5 μm^2 area. **b** The size distribution of the particles imaged in **a**. **c** High-resolution XPS analysis is showing the Zn $2p_{3/2}$ core line, with the Zn peak occurring at a binding energy of 1020.9 eV and the ZnO peak occurring at 1022.5 eV. (Permission from Dovepress # 11575629)

TEM

Zinc metal nanoparticles are shown in Fig. 2 as TEM micrographs. The TEM micrographs reveal nanoparticles with diameters of approximately 2–5 nm in size showing crystal lattice fringes.

Odorant responses

Representative EOG recordings (Fig. 3) show odorant responses modified by 1.2 nm zinc nanoparticles as well as small and large zinc oxide nanoparticles. The relative peak amplitudes are given in Table 1. Only non-oxidized zinc nanoparticles enhance odorant responses. The oxidized nanoparticles manifested a slight decrease of the EOG amplitude when they were mixed with odorants. The EOG signals evoked by ZnO nanoparticles with water vapor (no odorants) were minuscule and not much different from the EOG responses to water vapor (Table 1; Fig. 3, traces 5–7). The control experiments with respiratory epithelium show no response to the odorant and a mixture of odorant with zinc metal nanoparticles (Fig. 4).

Zn^{2+} ion concentration in suspensions of nanoparticles

The Zn^{2+} ion levels are given in Table 1. The Zn^{2+} ion concentrations are presented as mean values ± SD. The

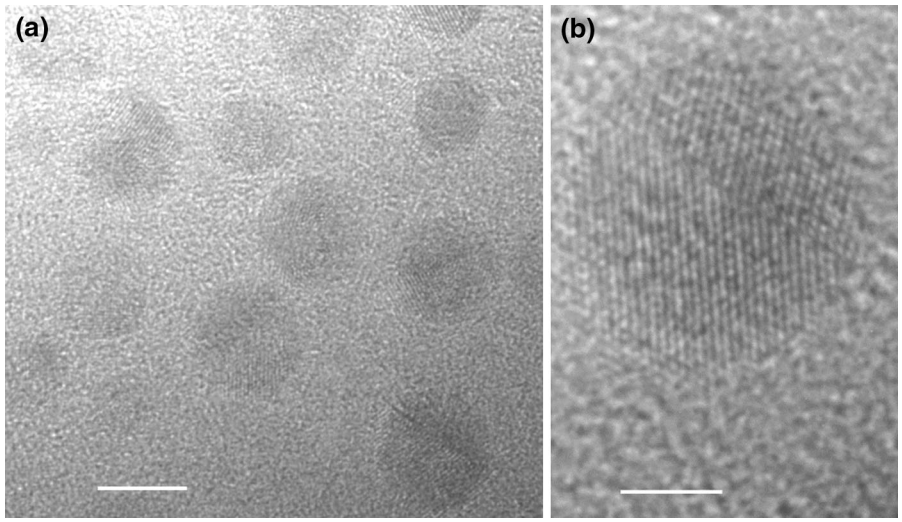

Fig. 2 Transmission electron microscopy of zinc metal nanoparticles. **a** *Bar* 5 nm. **b** *Bar* 2 nm

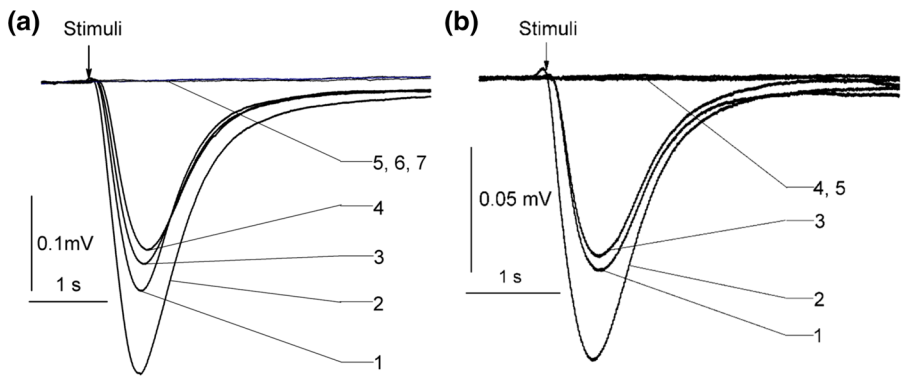

Fig. 3 Representative EOG recordings from rat olfactory epithelium. **a** The stimuli were of 0.25 s pulses of (*1*) odorant mixture, (*2*) odorant mixture +1.2 nm zinc nanoparticles, (*3*) odorant mixture + 15 nm ZnO nanoparticles, (*4*) odorant mixture + 70 nm ZnO nanoparticles, (*5*) 15 nm ZnO nanoparticles, (*6*) 70 nm ZnO nanoparticles, and (*7*) water vapor. The representative set of traces was obtained from 200 EOG traces. **b** The stimuli were of 0.25 s pulses of (*1*) odorant mixture, (*2*) odorant mixture +1.2 nm zinc nanoparticles, (*3*) odorant + 1.2 nm ZnO nanoparticles, (*4*, *5*) water vapor. This is a typical representation of 300 traces

zinc ion concentration in the suspension of 1.2 nm zinc nanoparticles is more than four times greater than that of 1.2 nm zinc oxide. The zinc ion concentration in all ZnO suspensions varies between 1 μmol/L and 13 μmol/L, while the relative amplitude of EOG evoked by the odorant + suspensions changes only by 0.1 %.

Discussion

Zinc plays the significant role in neurobiology (Frederickson et al. 2006). In most cases, the distribution of zinc in the brain was studied by methods that cannot discriminate between zinc ions and zinc metal particles (Takeda et al. 1997; Takeda 2001). Zinc is present in many regions of the CNS; it is found in particularly high concentrations in the olfactory bulb (OB) (Donaldson et al. 1973). The zinc content in whole rat blood is ≈100 μmol/L (Fugono et al. 2002), but Zn^{2+} ion concentrations in the neuronal extracellular fluid are estimated to be 0.15 μmol/L (Takeda 2000). The intracellular free Zn^{2+} ion concentration in neurons is estimated to be in the picomolar range and to fluctuate in this range

Table 1 Effect of nanoparticles on the odorant responses

Stimuli suspension[a]	Nanoparticle size (nm)	Relative amplitude[b]	(Zn^{2+} ion)[c] (μmol/L)
Zn + odorant	1.2	1.46 ± 0.032	4.8 ± 0.5
ZnO + odorant	1.2	0.82 ± 0.017	1.0 ± 0.20
ZnO + odorant	15	0.88 ± 0.014	7.7 ± 0.8
ZnO + odorant	70	0.85 ± 0.019	13.0 ± 2.0
ZnO with water vapor	15	0.0153 ± 0.004	7.7 ± 0.8
ZnO with water vapor	70	0.0226 ± 0.006	13.0 ± 2.0
Water vapor	NA	0.0360 ± 0.007	NA

[a] Excitation of EOG by 1.6 mm odorant vapor + 0.02 nmol/L of nanoparticles

[b] Relative amplitude of the EOG peak evoked by the stimuli to the EOG peak evoked by odorant alone (mean value ± SD)

[c] Concentration of Zn^{2+}ions in the stimuli suspension before application to olfactory epithelium (mean value ± SD). 1.2 nm ZnO nanoparticles were obtained by oxidation of 1.2 nm zinc nanoparticles

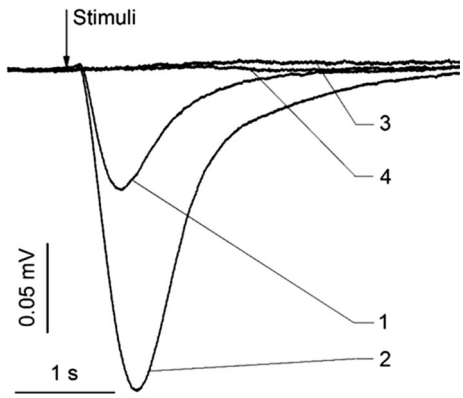

Fig. 4 Representative EOG recordings from rat olfactory and respiratory epithelia. The stimuli were of 0.25 s pulses of odorant with or without nanoparticles. (*1*) olfactory epithelium, odorant mixture, (*2*) olfactory epithelium, odorant mixture +1.2 nm zinc nanoparticles, (*3*) respiratory epithelium, odorant mixture, (*4*) respiratory epithelium, odorant mixture +1.2 nm zinc nanoparticles. The demonstrative set of traces was obtained from 200 EOG traces

(Bozym et al. 2006; Li et al. 2009). The physiological role of the endogenous Zn^{2+} ions in the olfactory sensory neurons is not very clear. However, added zinc ions at concentrations 20 μmol/L can inhibit the stimulatory GTP-binding protein of adenylyl cyclase (Gao et al. 2005), an important component of the initial events of olfactory signal transduction. The physiological role of endogenous Zn^{2+} ions is well studied in the neurons of the OB. Localized to synaptic terminals, zinc ions can be released by membrane depolarization and can reach extracellular synaptic concentrations of 100 μmol/L to 300 μmol/L. The released zinc modulates neuronal excitability under normal conditions (Horning et al. 2000; Horning and Trombley 2001).

The fact that the EOG responses to odorants are enhanced by the engineered 1.2 nm zinc nanoparticles is important because the small endogenous zinc nanoparticles are found in human and animal blood (Samoylov et al. 2005) and these naturally occurring nanoparticles also enhance olfactory responses (Viswaprakash et al. 2009).

Because, zinc nanoparticle enhancement was seen in awake animals (Jia et al. 2016) and both young and mature cell cultures (Viswaprakash et al. 2010), as well as in the dissected OE and that endogenous zinc nanoparticles are found in live animals' blood (Samoylov et al. 2005), this enhancement is significant for the initial events in olfaction.

Olfaction begins with sniffing, that transports odorant molecules into the nose and delivers them to the mucus layer covering the OE. The binding of the odorant to a receptor protein (Lancet and Pace 1987; Buck and Axel 1991) initiates an intracellular cascade of signal transduction events, including the G-protein-dependent production of second messenger molecules by adenylyl cyclase (Breer 2003a, b) leading to opening of ion channels and passing of ion currents (Zufall et al. 1991). This process triggers an action potential in the olfactory receptor neurons (ORNs) (Lancet and Benarie 1993) that projects directly to the OB (Harel et al. 2003). The signal is

then transmitted to the anterior olfactory nucleus, piriform cortex, periamygdaloid cortex, and entorhinal cortex via olfactory stria (Castiglioni et al. 2011). The phosphodiesterase activity in the cilia is accounted for rapid termination of the olfactory response by degrading odor-induced second messenger molecules (cAMP) (Firestein et al. 1991; Boekhoff and Breer 1992).

The enhancement of EOG responses to odorant by the zinc metal nanoparticles and inability to facilitate olfaction by addition to odorant zinc oxide nanoparticles may have a dual nature. The oxidation of zinc nanoparticles may change a physical state of the metal, but also could result in a production of zinc ions (Wöll 2007) that would inhibit olfactory responses. The inhibition by zinc ions may occur due to blocking cyclic-nucleotide-gated-channels (Kramer and Molokanova 2001), activation of cAMP-specific phosphodiesterase (Percival et al. 1997), inhibition of adenylyl cyclase (Klein et al. 2004) and $G_{\alpha s}$-protein (Gao et al. 2005). Our results, however, show no correlation between the relative amplitude of the EOG peak and the concentration of Zn^{2+} ions (Table 1). 1.2 nm zinc nanoparticles increase responses to odorant by a factor of 1.46 (Table 1). When these zinc nanoparticles were oxidized, they were not able to enhance responses to the odorant. This inability to enhance response to odorant is difficult to attribute to the inhibitory actions of zinc ions. The concentration of Zn^{2+} ions that go together with oxidized zinc nanoparticles is five times smaller than that accompanied non-oxidized zinc when the strong enhancement observed. Additionally, The Zn^{2+} ion concentration in all ZnO suspensions changes by 13 folds, while the relative amplitude of EOG evoked by the odorant + ZnO suspensions varies only by 0.1 %. These data suggest that after oxidation, the changed physical state of zinc rather than the changed valence state is a nature of the ZnO nanoparticles failure to enhance olfactory odorant responses.

The TEM images reveal round nanoparticles of various diameters. The high-resolution images of zinc metal nanoparticles show lattice fringes which indicate that zinc nanoparticles are crystals. Within the uncertainty of our measurements, we found that the typical fringes of 0.21 nm and 0.17 nm correspond to [01$\underline{1}$1] and [01$\underline{1}$2] directions for the hexagonal close-packed crystal lattice of metal zinc. The results are consistent with those obtained for zinc nanowires and nanorod (Chen et al. 2007; Lu et al. 2016).

The AFM and XPS spectra of small zinc nanoparticle reveal that they are 1.2 nm in diameter and consisted of more than 94 % of non-oxidized zinc atoms (Fig. 1).

The production of nanometer-sized metallic particles suggests the assembly of a significant number of metal atoms. The crystal structure of metallic zinc has a hexagonal close-packed lattice with a constant a = b = 0.266 and c = 0.495 nm. The unit cell contains 6 atoms and has a volume of 0.0912 nm^3 (Yoo and Wei 1967). The total volume of the 1.2 nm particle is

$$V_{\text{tot}} = \frac{4}{3}\pi(0.6)^3 = 0.904\,\text{nm}^3$$

Then, the total number of atoms in the 1.2 nm zinc nanoparticle is estimated to be

$$N_{\text{tot}} = \frac{0.904 \times 6}{0.0912} = 59\,atoms$$

One of the remarkable properties of small metal nanoparticles is their stability in water and blood plasma (Samoylov et al. 2005). It was discovered that metal nanoparticles with 13, 55, 147, 309, 561, and 923 atoms, so-called ''magic number'' of atoms, have added stability. These nanoparticles were designated as full-shell nanoparticles that are constructed by successively packed layers of metal atoms around a single metal atom (Aiken and Finke 1999; Khanna et al. 2002). The percolation of air through the suspension of 1.2 nm zinc nanoparticles for 20 min at 313.15 K caused a modest reduction of non-oxidized zinc atoms to 88 % showing a substantial resistance to oxidation. After 317 days of storage of 1.2 nm zinc nanoparticles at 278 K (5 °C), the relative atomic concentrations at the beginning and the end of storage did not change. A similar resistance to atmospheric oxidation was observed in the chemically synthesized metallic zinc nanocrystals explained in part by the unique crystalline surface properties of the anisotropic nanoparticles (Mai et al. 2013).

To estimate the number of atoms in the shell of 1.2 nm zinc nanoparticles we find the volume of the shell as a difference between V_{tot} and V_{core}, where

$$V_{core} = \frac{4}{3}\pi\left(0.6 - \frac{0.495}{2}\right)^3 = 0.183\ \text{nm}^3$$

$$V_{shell} = 0.904 - 0.183 = 0.721\ \text{nm}^3$$

Then the number of atoms in the shell,

$$N_{shell} = \frac{0.721 \times 6}{0.0912} = 47\ atoms$$

The number of atoms in the core

$$N_{core} = \frac{0.183 \times 6}{0.0912} = 12\ atoms$$

The estimated 12 atoms of the core and the total 59 atoms of the 1.2 nm zinc nanoparticle are in close agreement with the "magic number" full-shell nanoparticles with 13 and 55 atoms.

Each metal atom has the maximum number of nearest neighbors, which imparts some degree of extra stability to full-shell clusters (Jena et al. 1996; Aiken and Finke 1999).

The crystal structure of ZnO also has a hexagonal close-packed lattice with constants a = b = 0.325 and c = 0.520 nm. If we assumed the more prevalent form of ZnO with the urzite structure, than it has 2 Zn and 2 O atoms per unit cell, making a total of four atoms per cell and a volume of 0.0475 nm^3 (Morkoç and Özgur 2009). The fractions of surface atoms in ZnO nanoparticles are given in Table 2. It is clearly seen from the table, the smaller the size of the particle, the larger the fraction of atoms on the surface. The high surface to volume ratio in some nanoparticles is known to provide high chemical reactivity (Kruyt 1952; Thomas 1988; Matijevic and Goia 2007).

The surface atoms of the 1.2 nm zinc nanoparticle account for 80 % of all atoms, while the surface of the 15 nm zinc oxide nanoparticle contains only 10 % of all atoms (Table 2).

The high surface-volume ratio and fraction surface atoms are important to give a zinc nanoparticle the ability to bind olfactory receptor proteins and create dimers necessary for the active olfactory receptor-G-protein dimers (Vodyanoy 2010; Moore et al. 2012; Jia et al. 2016). Endogenous zinc nanoparticles supply a particular quantity of functional receptor dimers that can be activated by the odorant and take part in the generation of the olfactory signal. The remainder of the monomeric receptors remains largely inactive and do not contribute to the odorant-induced olfactory response. When the OE is exposed to a mixture of zinc nanoparticles and the same odorant, additional receptor dimers are made by joining pairs of previously unbound receptors. The appearance of new receptor dimers will then result in an increase of the odorant-induced olfactory response.

Olfactory receptors belong to the 7-transmembrane receptor superfamily of proteins that have seven domains spanning the plasma membrane seven times and coupled with G-proteins (Buck and Axel 1991). The thickness of the plasma membrane that structurally houses the receptor-G-protein complex is about 5 nm (Mitra et al. 2004). Envisioning that zinc nanoparticle (<5 nm) binds two of these complexes is completely compatible with this membrane topology. Hence, the high surface-to-volume ratio of the 1.2 nm zinc nanoparticles should render coupling between the two receptors very efficient.

Table 2 Properties of nanoparticles

Sample	Size, nm	S/V ratio nm^{-1}[a]	Total Number Of atoms	Number of atoms in shell	f[b]
Zn	1.2	5.00	59	47	0.80
ZnO	1.2	5.00	76	62	0.82
ZnO	15	0.399	148,820	15,021	0.1
ZnO	70	0.085	1.51245E7	342,800	0.023

[a] Surface to volume ratio

[b] Fraction of surface atoms

The fundamental mechanism of olfaction, is not fully understood. Presently, the most accepted theories of olfaction are either based on molecular shape (Moncrieff 1954; Amoore 1963) or on vibrational properties of molecules (Dyson 1938; Wright 1977; Turin 1996). The first approach, a so-called lock-and-key mechanism, assumes the shape of the molecule determines the characteristic odor. The other suggested that molecular vibrations are the basis for odor specificity in different molecules. In 2011 Franco et al. (Franco et al. 2011) demonstrated that fruit flies (*Drosophila melanogaster*) can differentiate between regular odorants and their deuterated isotopes. Two years later Gane et al. (Gane et al. 2013) reported that humans also are capable of discriminating musk molecules from their deuterated isotopes. As deuteration does not change the shape of a molecule, the lock-and-key model is insufficient to explain those findings. The shape and vibration modes are highly debated and require new experimental and theoretical data (Block et al. 2015; Turin et al. 2015).

The enhancement of the olfactory response by zinc nanoparticles is significant in consideration of the Luca Turin's vibrational model that suggests an inelastic electron tunneling spectroscopy (IETS) mechanism for discriminating odors (Turin 1996). In the IETS model, the odorant evokes inelastic tunneling of an electron between donor D and acceptor A inside of the receptor. The points D and A are different in energy by $\hbar\omega_o$ (phonon energy), to ensure that tunneling of an electron takes place only if the energy is absorbed by an odorant's phonon. Turin hypothesizes that electron tunneling results in the G-protein dissociation, which triggers the olfactory signal cascade. The model requires the existence of an active donor of electrons, and it is plausible to propose that zinc nanoparticles act as electron donors (Vodyanoy 2010; Brookes et al. 2012; Jia et al. 2016).

It had been predicted that nanoparticles within the diameter range 1–10 nm would likely exhibit quantum–mechanical properties (Alivisatos 1996). The arising physical properties are not those of bulk metal nor those of molecular compounds. However, these properties are highly determined by the particle size, interparticle distance, and shape of the nanoparticles (Brust and Kiely 2002). The quantum size effect is manifested if the de Broglie wavelength of the valence electrons is of the same order as the size of the particle itself. Subsequently, the particles act electronically as zero-dimensional quantum dots (or quantum boxes) highly relevant to quantum–mechanical principles. In nanoparticles, there is a gap between the valence band and the conduction band, in contrast to bulk metals. Single-electron tunnel transitions occur between a donor and acceptor, if the electrostatic energy, $E_{el} = e^2/2C$, is larger than the thermal energy, $E_T = kT$, where C is electric capacitance, e—elementary charge, k—Boltzmann coefficient, T—absolute temperature (Daniel and Astruc 2004). The capacitance of 2 nm metal particle, $C = 4\pi\varepsilon\varepsilon_o r$, where ε is the relative dielectric constant of the receptor protein, (Simonson and Brooks 1996), the ε_o is the vacuum dielectric constant 8.85×10^{-12}, and r = 1 nm. $C = 4\pi \times 9 \times 8.85 \times 10^{-12} \times 10^{-9} = 1.0 \times 10^{-18}$ F. $E_{el} = (1.6 \times 10^{-19})^2/(2 \times 1.0 \times 10^{-18}) = 1.15 \times 10^{-19}$ CV = 79.6 meV, that is considerably higher than the thermal energy at 25 °C, $E_T = 1.38 \times 10^{-23} \times 298 = 4.11 \times 10^{-21}$ J = 25.6 meV. Therefore, metal nanoparticles with a diameter smaller than 6 nm satisfy the condition of the single-electron transfer. The single-electron tunnel transition was experimentally observed with ~1 nm quantum dot at room temperature (Barreiro et al. 2012). The above considerations make the hypothesis of small zinc nanoparticles play a role of electron donors in Turin's model (Turin 1996) to be quite feasible.

Discontinuous size effects were experimentally observed in physics of small metal particles studied by the surface plasmon resonance, in the chemistry of supramolecular structures and molecular recognition, and in the biology of DNA-metal nanoparticle assemblies and sensors [reviewed in (Daniel and Astruc 2004)]. Based on this theoretical and known experimental evidence of the discontinuous size effects, we believe that our experimental results confirm the size influence and surface composition of zinc metal nanoparticles on the enhancement of olfactory odorant responses.

We found that zinc nanoparticles are involved in the initial event of olfaction—interaction with olfactory sensory receptors. However, the signal enhancement at this level is perceived by a central nervous system (Jia et al. 2014, 2016).

An evaluation of concentration dependency of odorant-stimulated olfactory sensory neuron shows

that One zinc nanoparticle binds Two receptor molecules to produce a dimer (Vodyanoy 2010). Additionally, there is useful information provided by immunoprecipitation, fluorescence resonance energy transfer, and bioluminescence resonance energy transfer (BRET) that's certainly a fraction of cilia olfactory receptors makes homodimers (Bush 2008; Hall 2009; Wade et al. 2011; Sanz and Pajot-Augy 2013) the same as the rhodopsin homodimerization in optic disc membranes discovered by AFM (Fotiadis et al. 2003a, b). We hypothesize that a single receptor cannot be stimulated by the odorant. Instead, only if it is coupled with another receptor with the assistance of a zinc nanoparticle, it can take part in signal transduction. It has been shown by immunogold electron microscopy that only a fraction of the olfactory receptors produces dimers, while all of those other receptors happen to be in the monomer state (Fukutani et al. 2012). Therefore, the enhancement of the olfactory signal by zinc nanoparticles could have a simple explanation. The endogenous zinc nanoparticles produce a particular quantity of operational receptor dimers that can be evoked by the odorant and take part in the origination of the olfactory signal. The rest of the monomeric receptors remain passive and do not input to the odorant-evoked olfactory response. If the OE is challenged with a mixture of zinc nanoparticles and the same odorant, new receptor dimers are made by connecting pairs of formerly unbound receptors. The input of new receptor dimers will then cause a rise of the odorant-evoked olfactory response.

Recently, zinc nanoparticles were shown to enhance rat olfactory odorant responses used in the bio-electronic nose (Zhang et al. 2016). Zinc nanoparticles are not only metal particles that are capable enhancing olfactory odorant response. Exposure to 0.45 μg/L nanosilver suspension led to increased Crucian carp EOG responses, whereas exposure to 45 μg/L silver nanoparticle suspension and silver ion solution resulted in suppressing EOG signals (Bilberg et al. 2011). Other studies confirm toxicity of silver nanoparticles and silver ions (Bilberg et al. 2010; Farmen et al. 2012). Intranasal zinc sulfate irrigation in mmol/L concentrations in rodents was shown to destroy olfactory receptors (Matulionis 1975; Burd 1993). In contrast, zinc nanoparticles did not manifest toxicity at the fractions of nmol/L concentrations are not toxic to astrocytes (Vodyanoy et al. 2016).

There are other methods to facilitate olfactory responses. Down-regulation of any step in the olfactory signal transduction cascade could contribute to termination of odorant-evoked responses. The receptor phosphorylation (Boekhoff and Breer 1992), inactivation of G-protein (Simon et al. 1991), reduction of adenylyl cyclase activity (Sklar et al. 1986), and activation of phosphodiesterase (Borisy et al. 1992) could cause a decrease in intracellular cAMP concentrations, and consecutively would reduce the olfactory response. Therefore, inhibition of this down-regulation would cause the enhancement of an olfactory response. Indeed, the existence of inhibitory $G_{\alpha i}$-subunits in olfactory cilia and the adenylyl cyclase enhancement in the presence of $G_{\alpha i}$-antibody were demonstrated (Sinnarajah et al. 1998). Similarly, the inhibition of RGS2 proteins downregulates signal transduction in olfactory neurons by inhibiting activation of adenylyl cyclase. The whole cell patch-clamp experiments demonstrated the enhancement of odorant responses by inhibition of RGS2 proteins by RGS2 antibodies (Sinnarajah et al. 2001). Also, the deactivation of the phosphodiesterase by the IBMX increased cAMP levels in olfactory cilia (Moore et al. 2012). The above enhancement methods are based upon the biochemical intervention that is difficult to implement in live animals. Whereas, the enhancement of odorant responses by zinc nanoparticles was demonstrated in fully unrestrained conscious dogs (Jia et al. 2016).

Disclaimer

Certain commercial equipment, instruments, or materials are identified in this paper to specify the experimental procedure adequately. Such identification is not intended to imply recommendation or endorsement by the National Institute of Standards and Technology, nor is it intended to imply that the materials or equipment identified are necessarily the best available for the purpose.

Conclusions

1. Transmission electron microscopy showed a crystalline structure of zinc metal nanoparticles.

2. Atomic force microscopy and X-ray photoelectron spectroscopy revealed that the majority of the zinc atoms of 1.2 nm zinc nanoparticles were not oxidized.
3. 1.2 nm zinc nanoparticles are suggested to serve as donors of electrons in Turin's vibrational model of olfaction.
4. After oxidation zinc, nanoparticles lose the ability to enhance responses to the odorant.
5. Zinc and zinc oxide nanoparticles do not evoke considerable responses in olfactory sensory neurons when delivered without odorants.

Acknowledgments The work was funded by NIST Grant: 70 NANB14H324

References

Aiken JD, Finke RG (1999) A review of modern transition-metal nanoclusters: their synthesis, characterization, and applications in catalysis. J Mol Catal A 145:1–44

Alivisatos AP (1996) Semiconductor clusters nanocrystals, and quantum dots. Science 271:933–937. doi:10.1126/science.271.5251.933

Amoore JE (1963) Stereochemical theory of olfaction. Nature 198:271–272

Barreiro A, van der Zant HSJ, Vandersypen LMK (2012) Quantum dots at room temperature carved out from few-layer graphene. Nano Lett 12:6096–6100. doi:10.1021/nl3036977

Bilberg K, Malte H, Wang T, Baatrup E (2010) Silver nanoparticles and silver nitrate cause respiratory stress in Eurasian perch (*Perca fluviatilis*). Aquat Toxicol 96:159–165. doi:10.1016/j.aquatox.2009.10.019

Bilberg K, Døving KB, Beedholm K, Baatrup E (2011) Silver nanoparticles disrupt olfaction in Crucian carp (*Carassius carassius*) and Eurasian perch (*Perca fluviatilis*). Aquat Toxicol 104:145–152. doi:10.1016/j.aquatox.2011.04.010

Black D, Ritter JJ, Bonevich JE, Henins A, Cline JP (2012) Nanocrystalline zinc oxide powder for x-ray diffraction metrology. Adv X Ray Anal 56:61–70

Block E, Jang S, Matsunami H, Sekharan S, Dethier B, Ertem MZ, Gundala S, Pan Y, Li S, Li Z, Lodge SN, Ozbil M, Jiang H, Penalba SF, Batista VS, Zhuang H (2015) Implausibility of the vibrational theory of olfaction. Proc Natl Acad Sci USA 112:E2766–2774. doi:10.1073/pnas.1503054112

Boekhoff I, Breer H (1992) Termination of second messenger signaling in olfaction. Proc Natl Acad Sci USA 89:471–474

Borisy F, Ronnett G, Cunningham A, Juilfs D, Beavo J, Snyder S (1992) Calcium/calmodulin-activated phosphodiesterase expressed in olfactory receptor neurons. J Neurosci 12:915–923

Bozym RA, Thompson RB, Stoddard AK, Fierke CA (2006) Measuring picomolar intracellular exchangeable zinc in PC-12 cells using a ratiometric fluorescence biosensor. ACS Chem Biol 1:103–111

Breer H (2003a) Olfactory receptors: molecular basis for recognition and discrimination of odors. Anal Bioanal Chem 377:427–433

Breer H (2003b) Sense of smell: recognition and transduction of olfactory signals. Biochem Soc Trans 31:113–116

Brookes JC, Horsfield AP, Stoneham AM (2012) The swipe card model of odorant recognition. Sensors 12:15709–15749. doi:10.3390/s121115709

Brust M, Kiely CJ (2002) Some recent advances in nanostructure preparation from gold and silver particles: a short topical review. Colloids Surf A 202:175–186. doi:10.1016/S0927-7757(01)01087-1

Buck L, Axel R (1991) A novel multigene family may encode odorant receptors—a molecular-basis for odor recognition. Cell 65:175–187

Burd GD (1993) Morphological-study of the effects of intranasal zinc-sulfate irrigation on the mouse olfactory epithelium and olfactory-bulb. Microsc Res Tech 24:195–213. doi:10.1002/jemt.1070240302

Bush CF (2008) Olfactory receptor dimerization. Ph D dissertation, Emory University. https://etd.library.emory.edu/view/record/pid/emory:15jh3

Castiglioni AJ, Remis NN, Flores EN, Garcia-Anoveros J (2011) Expression and vesicular localization of mouse Trpml3 in *Stria vascularis*, hair cells, and vomeronasal and olfactory receptor neurons. J Comp Neurol 519:1095–1114. doi:10.1002/cne.22554

Chen YJ, Chi B, Zhang HZ, Chen H, Chen Y (2007) Controlled growth of zinc nanowires. Mater Lett 61:144–147. doi:10.1016/j.matlet.2006.04.044

Cline JP, Leoni M, Black D, Henins A, Bonevich JE, Whitfield PS, Scardi P (2013) Crystalline domain size and faulting in the new NIST SRM 1979 zinc oxide. Powder Diffr 28:S22–S32. doi:10.1017/S0885715613001188

Daniel MC, Astruc D (2004) Gold nanoparticles: assembly, supramolecular chemistry, quantum-size-related properties, and applications toward biology, catalysis, and nanotechnology. Chem Rev 104:293–346. doi:10.1021/cr030698+

Daniels YC, MacCrehan WA, Vodyanoy V (2015) Characterization of olfactory-enhancing zinc metal nanoparticles. Paper presented at the IEEE international conference on nanotechnology, Rome, July 27–30

Donaldson J, St. Pierre T, Minnich JL, Barbeau A (1973) Determination of Na+, K+, Mg^2+, Cu^2+, Zn^2+, and Mn^2+ in rat brain regions. Can J Biochem 51:87–92

Dyson GM (1938) The scientific basis of odour. Chem Ind 57:647–651

Farmen E, Mikkelsen HN, Evensen O, Einset J, Heier LS, Rosseland BO, Salbu B, Tollefsen KE, Oughton DH (2012) Acute and sub-lethal effects in juvenile Atlantic salmon exposed to low mug/L concentrations of Ag nanoparticles. Aquat Toxicol 108:78–84. doi:10.1016/j.aquatox.2011.07.007

Firestein S, Darrow B, Shepherd GM (1991) Activation of the sensory current in salamander olfactory receptor neurons depends on a G protein-mediated cAMP second messenger system. Neuron 6:825–835

Fotiadis D, Liang Y, Filipek S, Saperstein DA, Engel A, Palczewski K (2003a) Atomic-force microscopy: rhodopsin dimers in native disc membranes. Nature 421:127–128

Fotiadis D, Liang Y, Filipek S, Saperstein DA, Engel A, Palczewski K (2003b) Is rhodopsin dimeric in native retinal rods? Reply. Nature 426:31

Franco MI, Turin L, Mershin A, Skoulakis EMC (2011) Molecular vibration-sensing component in *Drosophila melanogaster* olfaction. Proc Natl Acad Sci USA 108:3797–3802. doi:10.1073/pnas.1012293108

Frederickson CJ, Giblin LJ, Krezel A, McAdoo DJ, Mueller RN, Zeng Y, Balaji RV, Masalha R, Thompson RB, Fierke CA, Sarvey JM, de Valdenebro M, Prough DS, Zornow MH (2006) Concentrations of extracellular free zinc (pZn)(e) in the central nervous system of man, rat and rabbit during anesthesia, ischemia and reperfusion. Exp Neurol 202:523–523

Fugono J, Fujimoto K, Yasui H, Kawabe K, Yoshikawa Y, Kojima Y, Sakurai H (2002) Metallokinetic study of zinc in the blood of normal rats given insulinomimetic zinc(II) complexes and improvement of diabetes mellitus in type 2 diabetic GK rats by their oral administration. Drug Metab Pharmacokinet 17:340–347

Fukutani Y, Ishii J, Noguchi K, Kondo A, Yohda M (2012) An improved bioluminescence-based signaling assay for odor sensing with a yeast expressing a chimeric olfactory receptor. Biotechnol Bioeng 109:3143–3151. doi:10.1002/bit.24589

Gane S, Georganakis D, Maniati K, Vamvakias M, Ragoussis N, Skoulakis EM, Turin L (2013) Molecular vibration-sensing component in human olfaction. PLoS One 8:e55780. doi:10.1371/journal.pone.0055780

Gao XL, Du ZY, Patel TB (2005) Copper and zinc inhibit G alpha(s) function. J Biol Chem 280:2579–2586

Gu X-F, Furuharaa T, Zhang W-Z (2016) PTCLab: free and open-source software for calculating phase transformation crystallography. J Appl Crystallogr 49:1–8

Hall RA (2009) Olfactory receptor interactions with other receptors. Ann NY Acad Sci 1170:147–149

Harel D, Carmel L, Lancet D (2003) Towards an odor communication system. Comp Biol Chem 27:121–133

Horning MS, Trombley PQ (2001) Zinc and copper influence excitability of rat olfactory bulb neurons by multiple mechanisms. J Neurophysiol 86:1652–1660

Horning MS, Blakemore LJ, Trombley PQ (2000) Endogenous mechanisms of neuroprotection: role of zinc, copper, and carnosine. Brain Res 852:56–61. doi:10.1016/S0006-8993(99)02215-5

Jena P, Khanna SN, Rao BK (1996) Stability and electronic structure of cluster assembled materials. In: Sattler K (ed) Cluster assembled materials. Trans Tech Publications, Zurich, pp 1–25

Jia H, Pustovyy O, Waggoner P, Beyers R, Schumacher J, Barrett J, Morrison E, Gillette R, Denney T, Vodyanoy V, Deshpande G (2012) Functional MRI of the olfactory system in awake and anesthetized dogs. Paper presented at the 20th annual meeting of the International Society for Magnetic Resonance in Medicine, Melbourne

Jia H, Pustovyy OM, Waggoner P, Beyers RJ, Schumacher J, Wildey C, Barrett J, Morrison E, Salibi N, Denney TS, Vodyanoy VJ, Deshpande G (2014) Functional MRI of the olfactory system in conscious dogs. PLoS One 9:e86362. doi:10.1371/journal.pone.0086362

Jia H, Pustovyy OM, Wang Y, Waggoner P, Beyers RJ, Schumacher J, Wildey C, Morrison E, Salibi N, Denney TS, Vodyanoy VJ, Deshpande G (2016) Enhancement of odor-induced activity in the canine brain by zinc nanoparticles: a functional MRI study in fully unrestrained conscious dogs. Chem Senses 41:53–67. doi:10.1093/chemse/bjv054

Khanna SN, Rao BK, Jena P (2002) Magic numbers in metallo-inorganic clusters: chromium encapsulated in silicon cages. Phys Rev Lett 89:016803. doi:10.1103/PhysRevLett.89.016803

Klein C, Heyduk T, Sunahara RK (2004) Zinc inhibition of adenylyl cyclase correlates with conformational changes in the enzyme. Cell Signal 16:1177–1185

Kramer RH, Molokanova E (2001) Modulation of cyclic-nucleotide-gated channels and regulation of vertebrate phototransduction. J Exp Biol 204:2921–2931

Kruyt HR (1952) Colloid science, vol VI. Elsevier, New York

Lancet D, Benarie N (1993) Olfactory receptors. Curr Biol 3:668–674

Lancet D, Pace U (1987) The molecular-basis of odor recognition. Trends Biochem Sci 12:63–66

Li Y, Maret W (2009) Transient fluctuations of intracellular zinc ions in cell proliferation. Exp Cell Res 315:2463–2470

Lu C, Cheng Y, Pan Q, Tao X, Yang B, Ye G (2016) One-dimensional growth of zinc crystals on a liquid surface. Sci Rep 6:19870. doi:10.1038/srep19870

Mai NT, Thuy TT, Mott DM, Maenosono S (2013) Chemical synthesis of blue-emitting metallic zinc nano-hexagons. Cryst Eng Comm 15:6606–6610. doi:10.1039/C3CE40801A

Matijevic E, Goia D (2007) Formation mechanisms of uniform colloid particles. Croat Chem Acta 80:485–491

Matulionis DH (1975) Ultrastructural study of mouse olfactory epithelium following destruction by $ZnSO_4$ and its subsequent regeneration. Am J Anat 142:67–89. doi:10.1002/aja.1001420106

Mitra K, Ubarretxena-Belandia I, Taguchi T, Warren G, Engelman DM (2004) Modulation of the bilayer thickness of exocytic pathway membranes by membrane proteins rather than cholesterol. Proc Natl Acad Sci USA 101:4083–4088. doi:10.1073/pnas.0307332101

Moncrieff RW (1954) The characterization of odours. J Physiol 125:453–465

Moore CH, Pustovyy O, Dennis JC, Moore T, Morrison EE, Vodyanoy VJ (2012) Olfactory responses to explosives associated odorants are enhanced by zinc nanoparticles. Talanta 88:730–733. doi:10.1016/j.talanta.2011.11.024

Morkoç H, Özgur Ü (2009) Zinc oxide: fundamentals, materials and device technology. Wilay, Weinheim

Percival MD, Yeh B, Falgueyret J-P (1997) Zinc dependent activation of cAMP-specific phosphodiesterase (PDE4A). Biochem Biophys Res Commun 241:175–180

Samoylov AM, Samoylova TI, Pustovyy OM, Samoylov AA, Toivio-Kinnucan MA, Morrison NE, Globa LP, Gale WF, Vodyanoy V (2005) Novel metal clusters isolated from blood are lethal to cancer cells. Cells Tissues Organs 179:115–124

Sanz G, Pajot-Augy E (2013) Deciphering activation of olfactory receptors using heterologous expression in *Saccharomyces cerevisiae* and bioluminescence resonance energy transfer. Olfactory Recept Methods Protoc 1003:149–160

Simon MI, Strathmann MP, Gautam N (1991) Diversity of g-proteins in signal transduction. Science 252:802–808

Simonson T, Brooks CL (1996) Charge screening and the dielectric constant of proteins: insights from molecular dynamics. J Am Chem Soc 118:8452–8458. doi: 10.1021/ja960884f

Sinnarajah S, Ezeh PI, Pathirana S, Moss AG, Morrison EE, Vodyanoy V (1998) Inhibition and enhancement of odorant-induced cAMP accumulation in rat olfactory cilia by antibodies directed against Gas/olf- and Gai-protein subunits. FEBS Lett 426:377–380

Sinnarajah S, Dessauer CW, Srikumar D, Chen J, Yuen J, Yllma S, Dennis JC, Morrison EE, Vodyanoy V, Kehrl JH (2001) RGS2 regulates signal transduction in olfactory neurons by attenuating activation of adenylyl cyclase III. Nature 409:1051–1055

Sklar PB, Anholt RRH, Snyder SH (1986) The odorant-sensitive adenylate-cyclase of olfactory receptor-cells—differential stimulation by distinct classes of odorants. J Biol Chem 261:5538–5543

Takeda A (2000) Movement of zinc and its functional significance in the brain. Brain Res Brain Res Rev 34:137–148

Takeda A (2001) Zinc homeostasis and functions of zinc in the brain. Biometals 14:343–351

Takeda A, Ohnuma M, Sawashita J, Okada S (1997) Zinc transport in the rat olfactory system. Neurosci Lett 225:69–71

Thomas JM (1988) Colloidal metals—past, present and future. Pure Appl Chem 60:1517–1528

Tokushige M, Nishikiori T, Ito Y (2010) Plasma-induced cathodic discharge electrolysis to form various metal/alloy nanoparticles. Russ J Electrochem 46:619–626. doi: 10.1134/s1023193510060042

Turin L (1996) A spectroscopic mechanism for primary olfactory reception. Chem Senses 21:773–791

Turin L, Gane S, Georganakis D, Maniati K, Skoulakis EMC (2015) Plausibility of the vibrational theory of olfaction. Proc Natl Acad Sci USA 112:E3154. doi: 10.1073/pnas.1508035112

Viswaprakash N, Dennis JC, Samoylov AM, Josephson EM, Morrison EE, Vodyanoy V (2006) Enhancement of odorant-induced responses in olfactory receptor neurons by zinc nanoclusters. Paper presented at the Society for Neuroscience annual meeting, Atlanta, October 16, 2006

Viswaprakash N, Dennis JC, Globa L, Pustovyy O, Josephson EM, Kanju P, Morrison EE, Vodyanoy V (2009) Enhancement of odorant-induced response in olfactory receptor neurons by zinc nanoparticles. Chem Senses 34:547–557

Viswaprakash N, Josephson EM, Dennis JC, Yilma S, Morrison EE, Vodyanoy VJ (2010) Odorant response kinetics from cultured mouse olfactory epithelium at different ages in vitro. Cells Tissues Organs 192:361–373

Vodyanoy V (2010) Zinc nanoparticles interact with olfactory receptor neurons. Biometals 23:1097–1103. doi: 10.1007/s10534-010-9355-8

Vodyanoy V, Daniels Y, Pustovyy O, MacCrehan WA, Muramoto S, Stan G (2016) Engineered metal nanoparticles in the sub-nanomolar levels kill cancer cells. Int J Nanomed 11:1–10

Wade F, Espagne A, Persuy MA, Vidic J, Monnerie R, Merola F, Pajot-Augy E, Sanz G (2011) Relationship between homo-oligomerization of a mammalian olfactory receptor and its activation state demonstrated by bioluminescence resonance energy transfer. J Biol Chem 286:15252–15259. doi:10.1074/jbc.M110.184580

Wöll C (2007) The chemistry and physics of zinc oxide surfaces. Prog Surf Sci 82:55–120. doi: 10.1016/j.progsurf.2006.12.002

Wright RH (1977) Odor and molecular vibration: neural coding of olfactory information. J Theor Biol 64:473–502

Yoo MH, Wei CT (1967) Slip modes of hexagonal-close-packed metals. J Appl Phys 38:4317–4322. doi: 10.1063/1.1709121

Zhang Q, Zhang D, Li N, Lu Y, Yao Y, Li S, Liu Q (2016) Zinc nanoparticles-equipped bioelectronic nose using a microelectrode array for odorant detection. Anal Sci 32:387–393. doi:10.2116/analsci.32.387

Zufall F, Firestein S, Shepherd GM (1991) Analysis of single cyclic-nucleotide gated channels in olfactory receptor-cells. J Neurosci 11:3573–3580